fire

MDPI

Article

Drought and Wildfire Trends in Native Forests of South-Central Chile in the 21st Century

Efraín Duarte [1,2,*], Rafael Rubilar [1,2,3], Francisco Matus [4], Claudia Garrido-Ruiz [1,2,3], Carolina Merino [4,5], Cecilia Smith-Ramirez [6], Felipe Aburto [7], Claudia Rojas [8], Alejandra Stehr [9], José Dörner [10], Francisco Nájera [4,5], Guillermo Barrientos [11] and Ignacio Jofré [4,5]

1 Faculty of Forestry Sciences, Universidad de Concepción, Concepción 4070386, Chile; rafaelrubilar@udec.cl (R.R.); clagarrido@udec.cl (C.G.-R.)
2 Soil, Water, and Forest Research Laboratory (LISAB), Faculty of Forestry Sciences, Universidad de Concepción, Concepción 4070386, Chile
3 National Center of Excellence for the Wood Industry (CENAMAD), Pontifical Catholic University of Chile, Santiago 7820436, Chile
4 Laboratory of Conservation and Dynamic of Volcanic Soils, Department of Chemical Sciences and Natural Resources, Universidad de La Frontera, Temuco 4811230, Chile; francisco.matus@ufrontera.cl (F.M.); carolina.merino@ufrontera.cl (C.M.); francisco.najera@ufrontera.cl (F.N.); ignacio.jofre@ufrontera.cl (I.J.)
5 Geomicrobiology Laboratory, Department of Chemical Sciences and Natural Resources, Faculty of Engineering and Sciences, Universidad de la Frontera, Temuco 4811230, Chile
6 Department of Biological Sciences and Biodiversity, Universidad de Los Lagos, Osorno 5290000, Chile; cecilia.smith@ulagos.cl
7 Soil and Crop Sciences Department, Texas A&M University, College Station, TX 77843, USA; felipe.aburto@tamu.edu
8 Laboratory of Soil Microbial Ecology and Biogeochemistry (LEMiBiS), Institute of Agri-Food, Animal and Environmental Sciences (ICA3), Universidad de O'Higgins, San Fernando 3070000, Chile; claudia.rojas@uoh.cl
9 Faculty of Engineering, Universidad de Concepción, Concepción 4070386, Chile; astehr@udec.cl
10 Institute of Agrarian and Soil Engineering, Faculty of Agrarian and Food Sciences, Volcanic Soil Research Center, Universidad Austral de Chile, Valdivia 5110566, Chile; josedorner@uach.cl
11 Department of Civil Works, Faculty of Engineering Sciences, Universidad Católica del Maule, Talca 34809112, Chile; gbarrientos@ucm.cl
* Correspondence: efrainduarte@udec.cl

Abstract: Over the last decades, Chile has experienced a long-term drought with significant consequences for water availability, forest productivity, and soil degradation, ultimately dramatically increasing the surface of burned area. Here, we quantify the Palmer Drought Severity Index (PDSI) to ascertain the extent of "moisture deficiency" across the central-southern region of Chile from 2000 to 2023 to assess the drought's relationship with the frequency of wildfires focusing on the impact of native forests. Our methodology quantifies the PDSI from the burned area data using MODIS MCD64A1 satellite imagery, validated by in situ wildfire occurrence records. The findings indicate that 85.2% of fires occurred under moderate to severe drought conditions. We identified 407,561 ha showing varying degrees of degradation due to wildfires, highlighting the critical areas for targeted conservation efforts. A significant increase in both the frequency of wildfires and the extent of the affected area in native forests was observed with the intensification of drought conditions in the 21st century within mesic to humid Mediterranean climatic zones where drought explains up to 41% of the variability in the burned area ($r^2 = 0.41$; $p < 0.05$). This study highlights the relationship between drought conditions and wildfire frequency, showing the paramount need to adopt comprehensive wildfire mitigation management in native forests.

Keywords: drought; wildfires; native forest; remote sensing; climate change

Citation: Duarte, E.; Rubilar, R.; Matus, F.; Garrido-Ruiz, C.; Merino, C.; Smith-Ramirez, C.; Aburto, F.; Rojas, C.; Stehr, A.; Dörner, J.; et al. Drought and Wildfire Trends in Native Forests of South-Central Chile in the 21st Century. *Fire* **2024**, *7*, 230. https://doi.org/10.3390/fire7070230

Academic Editors: António Bento-Gonçalves, Luis A. Ruiz, Ting Yun and Fuquan Zhang

Received: 21 May 2024
Revised: 15 June 2024
Accepted: 16 June 2024
Published: 2 July 2024

1. Introduction

Wildfires' severity and frequency have increased in different regions of the world, strongly driven by changes in climatic conditions (including increased heat and extended drought) and leading to losses and degradation of forest ecosystems [1–4]. Between 26% and 29% of global forest losses from 2001 to 2019 were attributed to wildfires [5]. Recent extreme wildfires that occurred in Brazil, Australia, California [6], and Chile [1] emphasize the urgent need for a better understanding of the relationship between drought and forest fires as the drought periods have increased in frequency and severity in the 21st century.

In South-Central Chile (32–41°), there are regions most affected by forest wildfires with conditions varying from semiarid in the north to more mesic and humid conditions in the south [1], so Mediterranean vegetation such as shrublands and sclerophyllous forests and temperate deciduous forests (*Nothofagus* spp.) creates a landscape with one of the highest levels of fire activity in South America due to the region's abundant vegetative biomass and pronounced seasonal aridity [1,7]. In addition, the expansion of the extensive monoculture of exotic forest plantations in this area has further increased the accumulation of a higher fuel load [8,9].

South-Central Chile has experienced an uninterrupted climate characterized by below-normal precipitation since 2007, with mean rainfall deficits ranging between 20% and 31% (118 and 235 mm per year). This multiannual drought known as "Mega-Drought" coincides with the national warmest decade on record and an increase in the burned areas by forest fires [10–12]. In the last decade, Chile has experienced four globally extreme and historically anomalous fire disasters during the summers of 2015 and 2017, 2023, and recently 2024, burning together over 1 million hectares (ha) [13,14]. According to the public wildfire database reported by the National Forest Corporation (CONAF), in the 21st century, over 2 million ha have been disturbed by wildfires. Thus, the warmer and drier conditions in landscapes dominated by flammable and fuel-rich forest plantations might further promote catastrophic wildfires in South-Central Chile [7,14].

Over 90% of forest fires occur between 32° and 41° S latitude in the Mediterranean climate region [13]. This area is fire-prone due to hot, dry summers and cool, wet winters where forest wildfires have a positive significant relationship with the maximum temperature and winter precipitation in the year before the fire's occurrence. So, both drought and anomalously high moisture of the previous year control the fire regimes. However, the area affected by forest fires also depends on the fuel accumulation (biomass) and the summer drought that can dry out the biomass to become rapidly flammable [3,7,15].

The relationships between drought and forest fires are not an easy task, since direct and indirect drivers are involved. For example, human activity (which accounts for over 95% of the total ignitions) and vegetation type (land use change toward highly homogeneous exotic plantations and invasive shrubs and trees) are important factors to be considered [1,3,7,14].

Even though drought conditions have been associated with the increase in large wildfires' surface and a longer fire season [7], in Chile, studies targeting native forest vulnerability to fire under drought conditions have not been conducted. Native forests have a critical ecological role in providing essential ecosystem services such as water regulation, erosion control, and biodiversity conservation, and forest fires are one of the most devastating natural hazards; thus, the monitoring and prevention of forest fires are essential [16].

Furthermore, there are no up-to-date studies to assess the relationship between drought and fires considering the increase in the severity of the multiannual drought in the last 5 years and the future predictions of more recurrent and extended drought in South-Central Chile. Therefore, it is crucial to identify the regions more vulnerable to forest loss and degradation due to fire under this multiannual drought condition, where very large wildfires in forested ecosystems are predicted to increase as the effects of future drought [1,4,17].

Remote sensing technologies have become essential tools for monitoring, mapping, and assessing wildfires over large areas in a cost-effective manner [18,19]. Freely avail-

able multispectral and thermal sensors enable the assessment of soil moisture conditions, temperature, and vegetation health through the application of various vegetational indices [20,21], and has also significantly contributed to identifying fire risk, active fires, fire frequency, burn severity, and affected areas [22,23].

The Palmer Drought Severity Index (PDSI) is based on the difference between the amount of precipitation required to maintain a normal water balance and the actual amount of precipitation received [24] and is used to monitor drought conditions and as an important meteorological predictor for long-range wildfires; Zhao et al. (2021) [25] estimated the relationship between fire frequency and burned area using meteorological variables and various drought indices, finding significant correlations between annual fires and the PDSI. Donovan et al. (2020) [26] used the PDSI in the semi-arid regions of the western US to assess the relative dryness of an area and found that dryness at wildfire initiation averaged from Near Normal (a PDSI of −1.9 to 1.9) to Moderate Drought (a PDSI of −2.0 to −2.9); and Yang et al. (2023) [27] developed a series of multiple linear regression (MLR) models that linked the burned area with concurrent drought conditions, using the PDSI as a drought indicator for forecasting wildfires.

We hypothesize that the use of this index correlating the drought conditions with wildfire incidence across diverse ecosystems is suitable for our conditions, and the objectives of the present study were as follows: (i) to assess the relationship between drought and wildfires integrating remote sensing technologies and in situ forest fire data, (ii) to quantify the native forest affected by forest fires, and (iii) to identify the most vulnerable regions due to forest fires under these multiannual drought conditions in the 21st century.

2. Materials and Methods

This section provides a detailed description of the study area, the applied methodology, and the climatic, vegetation, and forest fire databases utilized, as well as the respective statistical analyses conducted to investigate the relationship between the drought severity and wildfire dynamics in the central-south macrozone of Chile.

2.1. Study Area

The research was conducted in the central-south macrozone of Chile, situated between latitudes 32° and 41° S, and includes the administrative regions from Valparaíso to Los Ríos (Figure 1). This region represents bioclimatic Mediterranean shrublands and north temperate forests, and the transition between Mediterranean and temperate oceanic climates [28]. This climatic variability has shaped the vegetation composition and structure, characterized by Mediterranean shrubs and temperate evergreen forests. The study area comprises approximately 2.9 million ha of exotic forest plantations, predominantly of *Pinus radiata* Don and in minor proportion Eucalyptus spp. and 4.6 million ha of remanent native forest [29]. Here, we focus on native forests only including both the Andes range and Coastal range.

The dominant native vegetation includes sclerophyllous shrubs, with representative species such as *Quillaja saponaria*, *Lithraea caustica*, and *Peumus boldus* [30]. Additionally, the study area hosts deciduous forests, primarily of the *Nothofagus* spp., and steppe vegetation at higher altitudes [31]. In regions with higher precipitation and humidity, extensive mixed temperate deciduous–evergreen forests are found, with dominant species like *Nothofagus obliqua*, *Nothofagus nervosa*, and *Nothofagus dombeyi* [32]. Above 1000 m above sea level (masl), the presence of *Araucaria araucana* stands out, occasionally mixed with other *Nothofagus* species such as *Nothofagus. pumilio* and *N. dombeyi* [33].

The administrative regions of Ñuble, Bíobío, and Araucanía feature vast extensions of forest plantations that provide an abundant and interconnected biomass, leading to an increased recurrence and severity of fires, especially during prolonged drought periods [7].

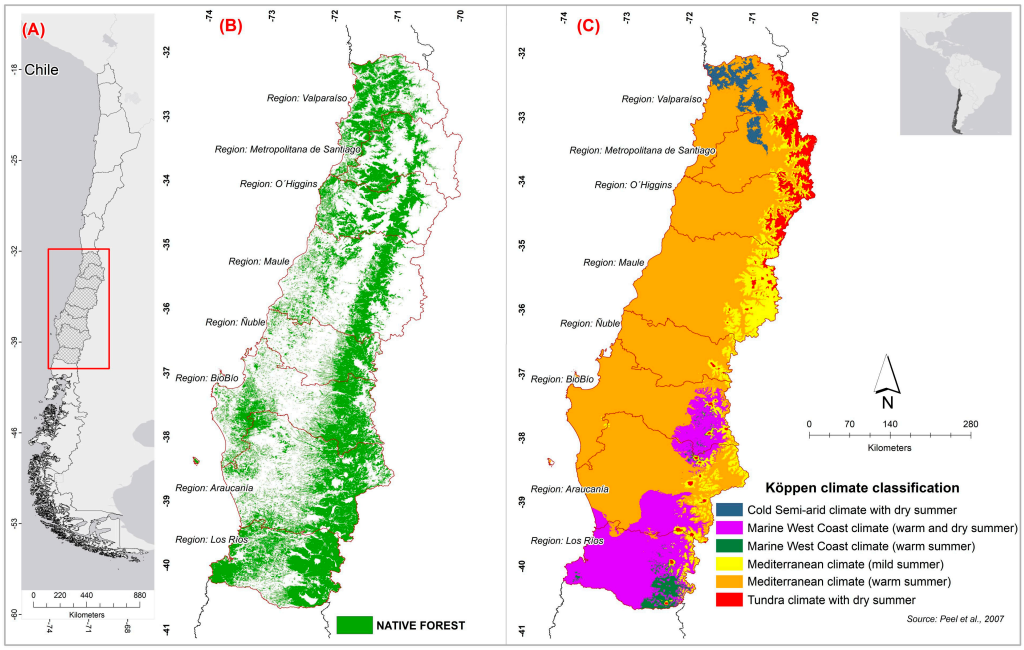

Figure 1. (**A**) Study area, (**B**) native forest and (**C**) Köppen climate classification (Peel et al., 2007) [28].

2.2. Methodology

The Google Earth Engine (GEE) cloud computing platform was utilized to process the data for this study [34]. The methodology consisted of four main steps, as illustrated in Figure 2. In the first step, satellite images from the MODIS Terra and Aqua combined MCD64A1 Collection Version 6.1 (2000–2023) were processed to identify and monitor the burned areas from forest fires (https://lpdaac.usgs.gov/products/mcd64a1v061/ accessed on 15 January 2024). This dataset provides comprehensive information on the extent and location of fire-affected areas, resulting in the creation of a geospatial forest fire database [35].

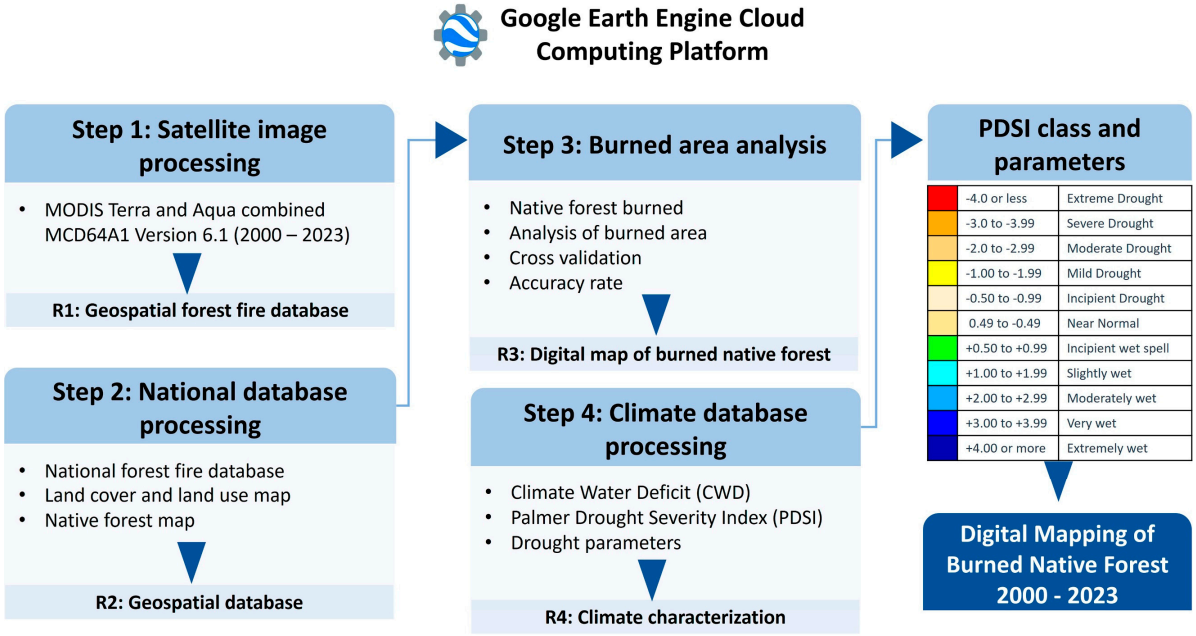

Figure 2. Methodological flowchart.

The second step involved processing national databases, including the national forest fire database, and land cover and land use maps. These data were used to validate the burned areas identified by the MODIS dataset and to provide comprehensive land cover information, resulting in a consolidated geospatial database.

In the third step, we analyzed the extent of the burned native forest areas. This analysis utilized the national forest wildfire database and the native forest map to quantify the extent of burned native forests. Cross-validation techniques were employed to ensure the accuracy of the burned area data, resulting in a digital map of burned native forest.

The fourth and final step involved processing the climate databases, including the PDSI [36], along with other drought parameters. A series of statistical analyses were conducted to determine the relationship between forest fires and long-term drought conditions. The PDSI provided a comprehensive evaluation of the intensity and frequency of extended periods of anomalously dry or wet conditions [37–39]. The PDSI data were used to explore the potential intensity of forest fires, resulting in a detailed climate characterization [40]. As a result, we obtained a spatially explicit digital map of native forests burned over the past 23 years in the south-central region of Chile. Table 1 provides a concise description of the main data utilized in the study, and Figure 2 shows a flow chart of the methodology employed. This structured approach allows for a detailed understanding of how increasing drought severity influences wildfire. Each step of the methodology is subsequently detailed in this section, providing a comprehensive overview of the processes and datasets involved in the study.

Table 1. Description of the main data applied in the study area.

Dataset	Type	Source	Applied in the Study [1]
Palmer Drought Severity Index (PDSI)	Raster Collection	ee.ImageCollection ("IDAHO_EPSCOR/TERRACLIMATE")	Drought severity
MODIS MCD64A1 version 6.1	Raster Collection	ee.ImageCollection ("MODIS/061/MCD64A1")	Monitoring the burned area
National forest fire database	Point	https://simef.minagri.gob.cl/ (accessed on 15 January 2024)	In situ wildfire data
Land cover map	Polygon	https://sit.conaf.cl/ (accessed on 15 January 2024)	Native forest cover land

[1] *Drought severity*: evaluated in the study area by soil moisture availability. *Monitoring the burned area*: to identify and monitor burned areas from fires (2000 to 2023), providing data on the extent and location of fire-affected areas. *In situ wildfire data*: in situ wildfire data were used to validate the burned areas identified by the MODIS. MCD64A1. *Land cover map*: used to map the native forest cover in the study area.

2.3. Geospatial Forest Fire Database

From January 2000 to April 2023, we used 273 satellite images from the MODIS instruments onboard NASA's Terra and Aqua combined MCD64A1 Version 6.1 [35] (https://lpdaac.usgs.gov/products/mcd64a1v061/ accessed on 15 January 2024). This is a monthly dataset with a spatial resolution of 500 m with per-pixel burned area and quality information. For burned area identification, the algorithm uses a burn-sensitive vegetation index (VI) to determine the dynamic thresholds within the data. This VI is derived from the MODIS shortwave infrared atmospherically corrected surface reflectance, specifically the implemented algorithm using spectral data derived from the red band (0.65 μm) that reflects chlorophyll absorption in healthy vegetation. The VI significantly decreases in burned areas due to the loss of live foliage. This results in a lower reflection in the red spectrum for burned versus unburned vegetation and infrared (1.24 μm and 2.13 μm) bands are associated with the cell structure of vegetation. Healthy vegetation reflects more in these infrared wavelengths due to the internal structure of leaves. When vegetation is burned, this structure is destroyed, leading to a significant reduction in infrared reflectance [35]. Figure 3 shows the spatial distribution of the burned area for the last 23 years.

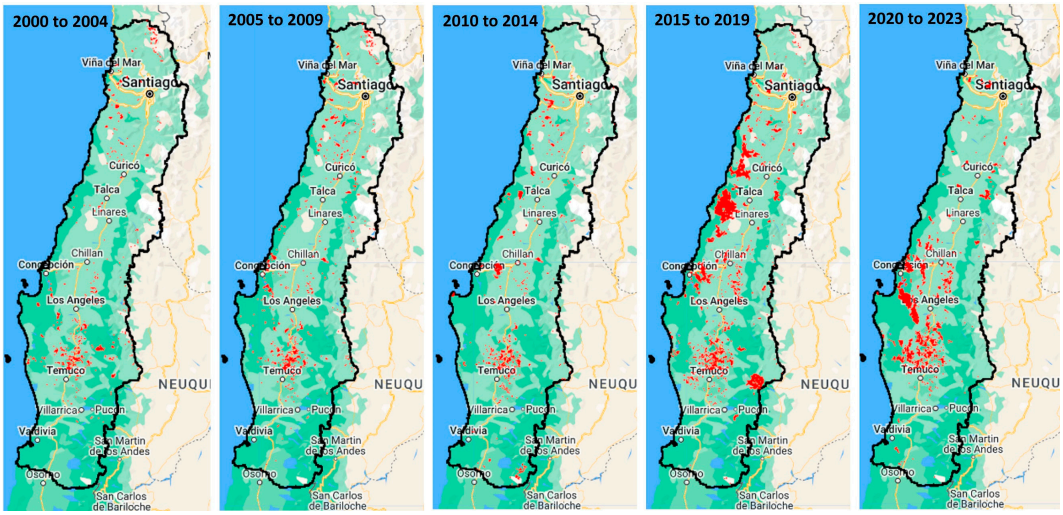

Figure 3. Spatial distribution of burned area in the 21st century from 2000 to 2023 from MODIS instruments onboard NASA's Terra and Aqua combined MCD64A1 Version 6.1 in central-south Chile (red color polygons indicate burned areas). (1 January start date and 31 December end date).

2.4. National Forest Wildfire Database

We employed the historical official database of forest fires from CONAF of the Chilean Native Forest Ecosystem Monitoring System (SIMEF) platform (https://simef.minagri.gob.cl/ accessed on 15 January 2024).

We used more than 9000 data points of native forest wildfires reported by CONAF in the last 23 years (Figure A1, Appendix A). This dataset encompasses the fire's date, causative factors, and geographic coordinates of the fire's location (points). These national records were used for validating forest fires mapped by the MODIS Terra and Aqua combined MCD64A1 Version 6.1 collection. We used these data due to the current unavailability of any official historical geospatial database of forest fires that delineates the areas affected by fires (polygons).

2.5. Climate Data

The dataset used contained 23 years of long monthly series of air temperature and atmospheric precipitation (climate and water balance) from the TerraClimate collection, and it was retrieved from the GEE platform. TerraClimate is a dataset of the high-spatial-resolution (1/24°, ~4-km) monthly climate and climatic water balance for global terrestrial surfaces from 1958 to the present.

In selecting the Palmer Drought Severity Index (PDSI) [24], we accurately considered its established reliability and widespread application in drought research globally. The PDSI, due to its comprehensive integration of moisture supply and demand factors—including rainfall and evapotranspiration—coupled with its capacity to simulate soil water content based on homogenized monthly temperature and precipitation data, presents a robust framework for quantifying drought severity [41,42]. Despite its advantages, we acknowledge the PDSI's potential limitations, such as its sensitivity to climatic and environmental parameters varying geographically and temporally [3,27].

Palmer (1965) [24] determined that drought severity could be effectively represented by four distinct classes, namely mild, moderate, severe, and extreme by assigning values to these classes based on 12 months of cumulative plots. The four classes of drought are separated from the opposite classes of wetness by normal conditions. The US National Oceanic and Atmospheric Administration classifies them into indices between 4 and −4 [39]. An index value of −4 represents extreme drought conditions, whereas a value of +4 indicates extremely wet conditions [43]; the PDSI ranges are shown in Figure 2 (methodological flowchart). The PDSI index is based on the difference between the amount of precipitation

required to maintain a normal water balance and the actual amount of precipitation received and facilitates comparisons across different periods and geographic regions [44]. The PDSI dataset used comes from *ee.ImageCollection("IDAHO_EPSCOR/TERRACLIMATE")* allocated in the GEE platform [34]. TerraClimate is a dataset of monthly climate and climatic water balance for global terrestrial surfaces; more information about this dataset is available in Abatzoglou et al. (2018) [37].

Therefore, from the literature review, we found alternative indices such as the Climate Water Deficit (CWD) [45], Standardized Precipitation Index (SPI) [46], Standardized Precipitation Evapotranspiration Index (SPEI) [47], and Palmer Modified Drought Index (PMDI) [48]. However, given the PDSI's proven efficacy in historical drought analysis and its specific applicability to our study region's climatic conditions, it was selected as the most suitable metric. Figure A1—Appendix A shows a map of the PDSI with the respective forest wildfires identified in situ.

2.6. Land Cover Data

The native forest map used in this study was derived from the Inventory of Native Vegetational Resources of Chile (in Spanish "Catastro Vegetacional"). This represents the foremost, ongoing public national initiative aimed to provide information on land use, with a specific focus on characterizing and locating the different native forests existing in the country [49].

The Catastro Vegetacional encompasses a standardized database, which facilitates efficient management and prompt information updates. It is publicly accessible and available for download via CONAF's Territorial Information System platform at https://sit.conaf.cl accessed on 15 January 2024.

2.7. Statistical Analysis

To assess the relationship between the PDSI and fire frequency and area burned, we used three drought periods: 2000–2007, 2007–2019, and 2019–2023. The 2000–2007 period served as a pre-drought baseline, while the 2007–2019 and 2019–2023 periods represent escalating drought conditions ending in severe drought. For this study, we subdivided the analysis into three distinct time periods to perform a structured temporal analysis. This approach allowed us to identify the correlation more clearly between increasing drought severity and the rise in both the frequency and magnitude of wildfires within the study area. By employing this method, we addressed the critical gap in understanding the relationship between drought severity, as measured by the PDSI, and the wildfire dynamics across different temporal scales. This structured temporal analysis provides novel insights into how escalating drought conditions relate to wildfire, which is essential for developing more effective fire management and mitigation strategies.

Thus, we compared the annual number of fires and area (ha) burned for each period using the Analysis of Variance (ANOVA) and Least Significant Difference (LSD) test.

The number of fires and burned area was assessed for different fire size classes: (i) 1–50 ha, (ii) 50–100 ha, (iii) 100–1000 ha, and (iv) >1000 ha [1].

The PDSI was evaluated as the annual mean, spring mean, summer mean, annual maximum, annual minimum, annual median, annual standard deviation, and the difference between the summer and spring PDSI. Pearson correlation was conducted between all these PDSI variations and area burned for fires from 1–1000 ha in size, as well as for each of the fire size classes to establish the basic associations between drought and wildfires. For all significant correlations, a regression analysis was performed to assess the strength and direction of the relationship between drought and wildfires.

3. Results

This section presents the findings of our study, organized into three main subsections to provide a comprehensive understanding of the data and analyses conducted. First, we detail the results regarding native forests affected by fires; this is followed by an analysis of

the drought conditions identified during the period from 2000 to 2023. Finally, we present the long-term drought trends in central-south Chile and their relationship with wildfires in native forests.

3.1. Drought and Native Forests Affected by Fires

For from 2000 to 2023, we used the PDSI as a relevant indicator to evaluate the drought conditions in various regions of central-southern Chile. According to the findings, 85.2% of fires occurred during periods of a moderate and severe PDSI index (Figure 4).

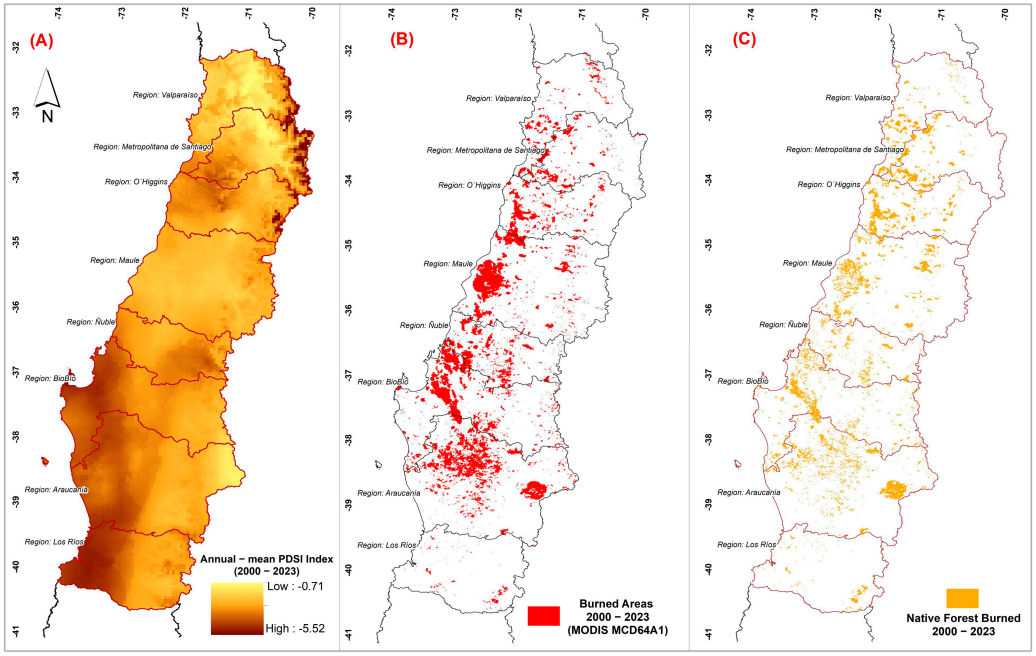

Figure 4. (**A**) Annual mean Palmer Drought Severity Index (PDSI) for season 2000−2023, (**B**) burned area from MODIS collection, and (**C**) native forest burned areas for season 2000−2023.

The maximum PDSI values were found in the Metropolitana Region with the most severe maximum PDSI (−5.52 extreme drought) and a minimum of −0.71 (mid drought), with an annual mean of −2.38, indicating significant variability. That for Valparaíso Region equaled the maximum PDSI in Santiago. Additionally, Ñuble presents the highest minimum PDSI (−2.16) and one of the lowest annual averages (−2.61), suggesting a more constant drought. The regions of Maule, La Araucanía, Biobío, and Los Ríos also showed a severe PDSI, with annual averages ranging between −2.25 and −2.86, reflecting a general situation of significant drought in these areas (Table 2).

Table 2. Annual mean Palmer Drought Severity Index (PDSI) metrics and Native Forest burned between 2000 and 2023.

Region	PDSI Max	PDSI Min	PDSI Mean	PDSI Std	Native Forest (ha)	Native Forest Burned (ha)	Native Forest Burned (%)
Metropolitana	−5.52	−0.71	−2.38	0.71	364,716	57,950	15.9%
O'Higgins	−4.96	−1.75	−2.53	0.36	460,052	70,786	15.4%
Maule	−3.37	−1.85	−2.25	0.17	582,214	72,733	12.5%
La Araucanía	−3.38	−1.23	−2.65	0.43	962,221	98,226	10.2%
Valparaíso	−5.52	−1.23	−2.11	0.50	484,778	43,450	9.0%
Biobío	−3.89	−1.75	−2.76	0.35	597,201	36,355	6.1%
Ñuble	−3.15	−2.16	−2.61	0.21	247,861	14,663	5.9%
Los Ríos	−3.55	−2.11	−2.86	0.43	907,327	13,398	1.5%
Total					**4,606,369**	**407,561**	**8.8%**

We evaluated 4.6 million ha of native forest within the regions, and we identified 407,561 ha (8.8%) of the native forest as being affected by fires for the 2000–2023 period. The administrative region with the highest percentage of native forest burned was Metropolitana with 15.9%. The most extensive area of native forest affected by wildfires was La Araucanía, which encompassed 98,226 ha (Table 3; Figure 4).

Table 3. Large-scale fires (>200 ha) per fire season for the study area reported by CONAF.

Fire Season	Number of Large-Scale Fires	Burned Area (ha)	
		Native Forest	Total
2002–2003	3	1865	6802
2003–2004	8	2881	9393
2004–2005	8	3147	10,272
2005–2006	2	400	1070
2006–2007	2	753	3071
2007–2008	2	2161	7340
2008–2009	8	6638	11,301
2009–2010	14	5833	21,554
2010–2011	9	4431	12,765
2011–2012	7	4404	36,943
2013–2014	15	13,389	31,922
2014–2015	16	23,541	45,044
2015–2016	2	557	1300
2016–2017	49	82,206	474,268
2018–2019	11	3867	11,736
2019–2020	11	13,203	28,915
2020–2021	5	3594	7195
2021–2022	10	5912	37,674
2022–2023	50	57,761	304,244

The MODIS MCD64A1 data for wildfire seasons in central-southern Chile between 2000 and 2023 show a significant inter-annual variability of wildfires, with some years exhibiting markedly high numbers. It is worth noticing that the 2016–2017 and 2022–2023 seasons stand out with 100,158 and 72,926 ha severely burned, respectively (Figure 5).

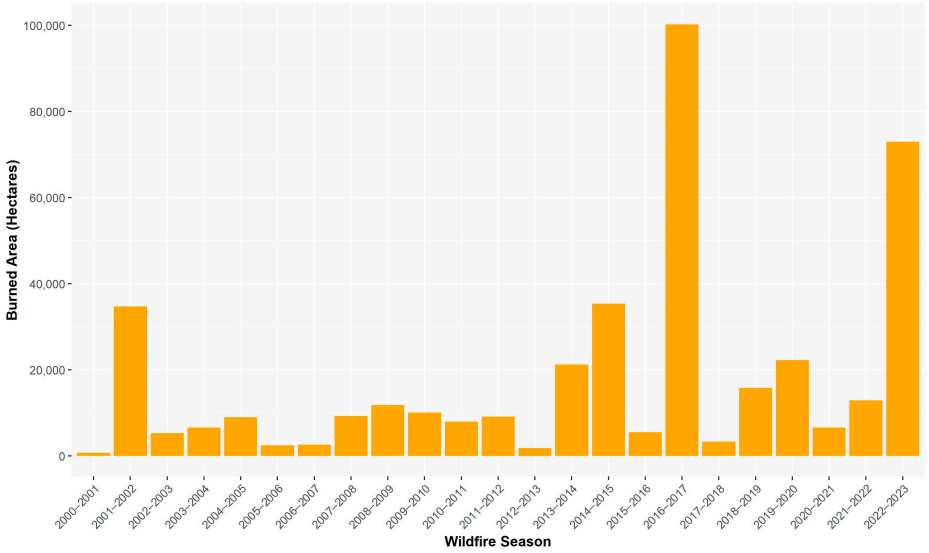

Figure 5. Annual burned area in native forest from MODIS MCD64A1 collection (2000–2023).

We found that these seasons are associated with extreme drought conditions, as suggested by the PDSI (see next subsection). Conversely, the seasons before a drought such

as 2002–2003 and 2005–2006, present the lowest areas affected, with less than 2500 ha each (Figure 6). The data present an upward trend in the area affected by wildfires over the two-decade span, with the latter half showing more frequent high-intensity events.

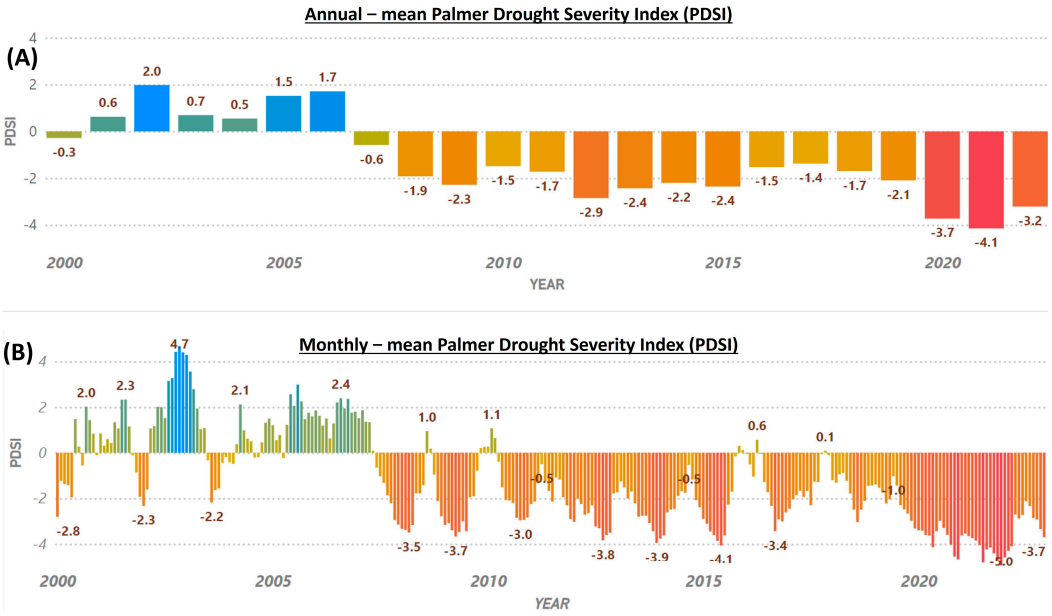

Figure 6. (**A**) Annual—mean Palmer Drought Severity Index (PDSI): 2000−2023 and (**B**) Monthly—mean PDSI 2000−2023.

We evaluated the accuracy of our reports using more than 9000 forest fire points from in situ data. Our results achieved high levels of spatial and temporal accuracy; we conducted cross-validation between areas identified as fires by the MCD64A1 Collection Version 6.1 from January 2000 to April 2023 versus fire points collected in situ during the same period; we found an 86.6% match, and the remaining 13.4% were false positives. The differences between these two data sources can be attributed to various factors. For instance, the resolution of the satellite data compared to on-site evaluations. Moreover, the differences can also be attributed to the field fire location with a single geographic coordinate, and an estimation of the affected surface was conducted by touring the affected area. This method for a scale fire > 200 ha can generate significant differences between the in situ estimated surface and that obtained through satellite data.

Large-scale fires are events characterized by complex interactions between extreme climatic conditions and catastrophic fires, which have become an increasing concern globally [50,51]. In Chile, CONAF defines a large-scale fire based on its significant social, economic, and environmental impacts, and by an affected area exceeding 200 hectares [13].

The data presented in Table 3 reveal a significant increase in both the frequency and the impact of large-scale fires on native forests and total burned areas across various seasons. Particularly, the fire seasons of 2016–2017 and 2022–2023 stand out for their extraordinary number of large-scale fires and the extensive areas affected, with over 82,206 ha and 57,761 ha of native forest burned, respectively.

We analyzed the native forests affected by fires according to their growth state. La Araucanía Region showed the largest burned area (98,226 ha), with early and late successional forests being the most affected, accounting for 30,786 ha and 48,761 ha, respectively. In contrast, the Maule Region demonstrated significant damage, predominantly concentrated in early successional forests (70,139 ha out of a total of 72,733 ha affected), which could have critical implications in terms of forest regeneration and biodiversity reduction (Table 4).

Table 4. Growth status of the native forest affected by forest fires in the period 2000–2023 and percentage (%) of native forest affected by administrative region of central-south Chile.

Region	Sclerophyllous Scrubs Forests		Late Successional Forest		Early/Late Successional Forest		Early Successional Forest		Total	
	ha	%	ha	%	ha	%	ha	%	ha	%
Metropolitana	0	0%	0	0%	1005	6%	56,945	16%	57,950	15.9%
O'Higgins	289	27%	1518	22%	2025	12%	66,954	15%	70,786	15.4%
Maule	591	4%	633	5%	1370	7%	70,139	13%	72,733	12.5%
La Araucanía	9241	11%	30,786	11%	9439	8%	48,761	10%	98,226	10.2%
Valparaíso	0	2%	0	0%	0	0%	43,450	9%	43,450	9.0%
Biobío	1331	3%	1701	2%	2050	4%	31,273	7%	36,355	6.1%
Ñuble	357	1%	843	9%	207	2%	13,257	7%	14,663	5.9%
Los Ríos	1595	4%	6002	1%	2168	2%	3633	1%	13,398	1.5%
Total	**13,404**	**6%**	**41,483**	**5%**	**18,264**	**5%**	**334,410**	**10%**	**407,561**	**8.8%**

3.2. Long-Term Drought in Central-South Chile

The assessment of the PDSI from the year 2000 to 2023 revealed notable fluctuations in drought conditions, with a striking trend towards drier conditions in recent years observed (a PDSI range of −4 to +4 where −4 indicates extreme drought and +4 extremely wet, but more extreme values are possible (see Figure 2 for the PDSI class and parameters)).

In the period 2000 to 2006, the annual mean PDSI values oscillated between −0.285 and 1.710, generally indicating wetter conditions or less severe droughts. However, starting in 2007, the situation worsened, with the PDSI displaying a pronounced negative trend, indicating an increase in drought severity. Particularly extreme is the period 2019–2023, where PDSI values reached indices with means up to the annual mean of −4.14 in 2021, suggesting extreme drought conditions (Figure 6A). Figure A2—Appendix B shows the PDSI values for each region for the years 2000 to 2023.

3.3. Relationship between the PDSI and Native Forest Fire

We conducted a temporal analysis of wildfire dynamics within the study area, revealing the significant changes in the extent of wildfires affecting native forests across different periods. During the pre-drought period of 2000 to 2007, we found that the annual average area impacted by wildfires was 12,845 hectares. In contrast, the subsequent long-term drought period from 2007 to 2023, where the annual average area burned, rose to 30,780 ha (refer to Figures 5 and A1—Appendix A for detailed insights into the affected area and its location).

The relationship between the increase in fire frequency and burned area with a long-term drought was analyzed for the three periods with increasing PDSI severity: (i) 2002–2007 (no drought) with a mean annual PDSI of 1.25 ± 1.39 and a summer PDSI of 1.49 ± 0.18, (ii) 2007–2019 (mild drought) with a mean annual PDSI of −1.64 ± 1.20 and summer PDSI of −1.80 ± 0.33, and (iii) 2019–2023 (severe drought) with a mean annual PDSI of −3.57 ± 0.67 and summer PDSI of −3.92 ± 0.39.

Overall, according to the LSD test, there was a significant increase in the burned area and the frequency of fires as the PDSI became more severe for fires of 1–50 ha size, whereas for fires between 50 and 1000 ha, the increase was only significant between the period 2002–2007 (no drought) and the most severe drought period (2019–2023) (Figure 7). Only four regions showed significant differences among the periods analyzed for burned area and fire frequency: La Araucanía, Biobío (including the Ñuble Region that before 2017 was a province of Biobío), and Maule.

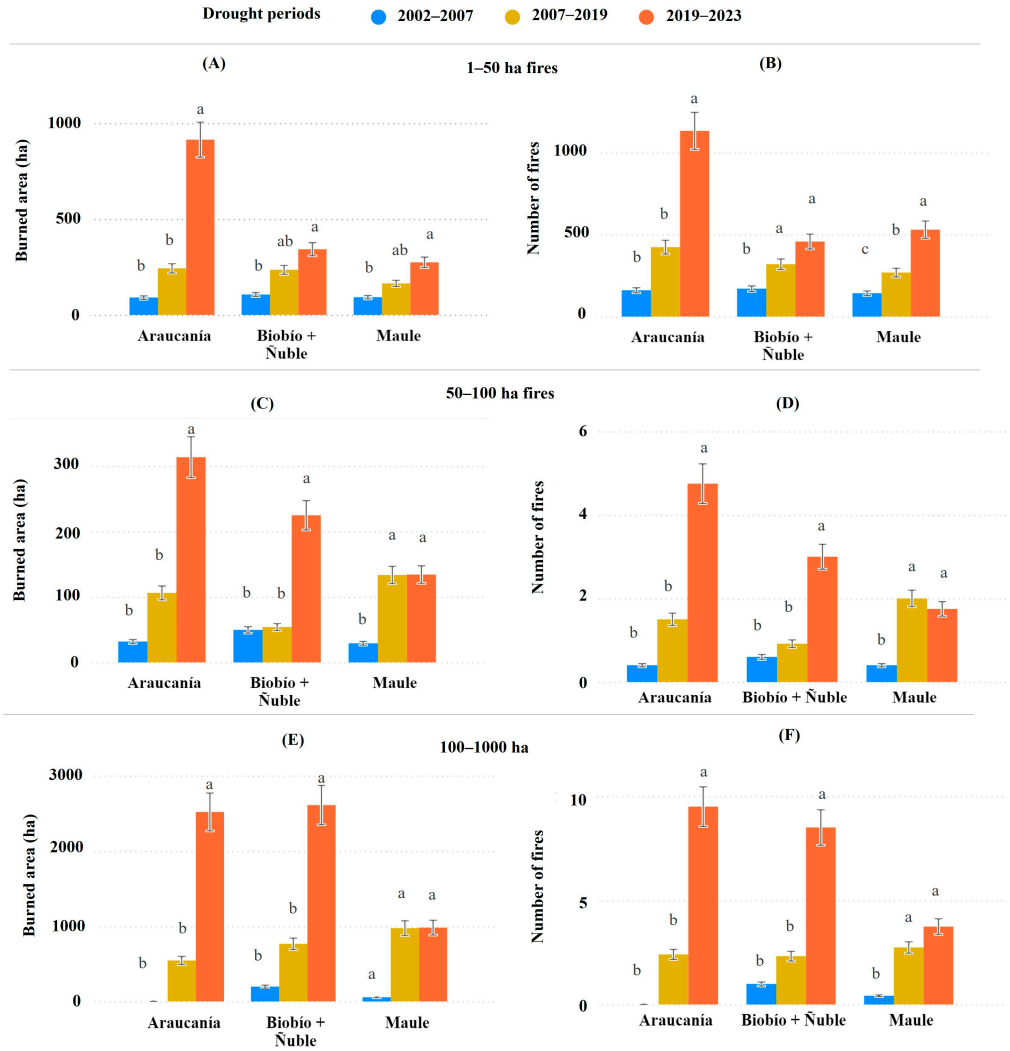

Figure 7. Annual mean burned area (ha) and number of fires according to the fire size classes. Blue bars represent mean annual values for the period 2002−2007 (no drought), yellow bars represent mean annual values for the period 2007−2019 (mild drought), and orange bars represent the mean annual value for the period 2019–2023 (severe drought). (**A**) Burned area of 1−50 ha fires per region; (**B**) Number of fires of 1–50 ha per region; (**C**) Burned area of 50−100 ha fires per region; (**D**) Number of fires of 50–100 ha per region; (**E**) Burned area of 100−1000 ha fires per region; and (**F**) Number of fires of 100–1000 ha per region. *Different letters above the bars represent statistically significant differences between study periods according to LSD test ($p < 0.05$).*

Although La Araucanía and Biobío showed greater PDSI severity periods, these values were only significant for the 2019–2023 period for fires from 1 to 1000 ha. Contrastingly, for the Maule Region, the significant increase in the fire burned area and frequency was observed in the period 2007–2019 with no differences between the last two periods (Figure 7). Particularly, the Maule Region, after seven years of continuous drought (2008–2015) that limited the fine fuel growth, there were nine months of incipient to moderate wetness the year before the native forest fires (2016) that promoted rapid growing and drying fuels in forest understories and grassland, followed by a severe spring drought (−3.15) and moderate summer drought (−2.97) (2016–2017), was the most affected region with the worst native forest fires on record that took place in January 2017. Thus, the summer of 2016–2017 with a moderate drought in Maule (−2.97), Biobío (−2.25), and O'Higgins Region (−2.37) exhibited a burned area of 67,367 ha of native forest affecting about 80% of the native forest burned during that fire season. Thus, this season represents the worst fire

event of the 21st century. Despite the nine months of wetness, Maule, along with Biobío and Ñuble were the only regions where the mean maximum monthly PDSI for the period (2007–2019) was negative with a mean summer PDSI of −2.13 and −2.26, respectively (moderate drought).

Regarding the last four years (2019–2023), the summers in Maule and La Araucanía experienced severe drought (a mean PDSI of −3.95 and −3.30, respectively). The change from moderate drought (2007–2019) to severe drought (2019–2023) increased the number of fires and burned area of 1–50 ha size fires in Maule with no difference in fires larger than 50 ha. For La Araucanía, this same change increased the area and number of fires from 1–1000 ha. This different response might be related to the precipitation in Maule being about half of La Araucanía thereby limiting the fuel production and preventing native forest fires with more severe drought (Figure 7).

Forest fires (1–1000 ha size) correlated better with the summer PDSI in Maule (r = −0.27; $p = 0.025$) and Biobío and Ñuble (r = −0.23; $p = 0.054$), whereas in La Araucanía, the maximum PDSI exhibited the best correlation (r = −0.38; $p < 0.001$). For these four regions, there was a negative correlation where a lower PDSI (more severe drought) was associated with a greater burned area. Contrarily, for the Los Ríos Region, the annual maximum PDSI (less severe drought) was positively associated with the annual burned area (r = 0.34; $p = 0.009$) (Table 5).

Table 5. Pearson correlation between the annual burned area from 1–1000 ha size fires and PDSI variables.

Pearson Correlation				
Region	**Mean Annual Burned Area**	**PDSI**	**r**	***p*-Value**
Los Ríos	**1–1000 ha fires**	**Maximum**	**0.34**	**0.009**
Araucanía	1–1000 ha fires	Annual	−0.36	0.0028
Araucanía	1–1000 ha fires	Spring	−0.29	0.017
Araucanía	1–1000 ha fires	Summer	−0.34	0.003
Araucanía	**1–1000 ha fires**	**Maximum**	**−0.38**	**0.001**
Araucanía	1–1000 ha fires	Minimum	−0.29	0.015
Araucanía	1–1000 ha fires	Median	−0.30	0.011
Biobío + Ñuble	1–1000 ha fires	Annual	−0.22	0.073
Biobío + Ñuble	**1–1000 ha fires**	**Summer**	**−0.23**	**0.054**
Biobío + Ñuble	1–1000 ha fires	Maximum	−0.21	0.080
Biobío + Ñuble	1–1000 ha fires	Minimum	−0.22	0.074
Maule	1–1000 ha fires	Spring	−0.23	0.057
Maule	**1–1000 ha fires**	**Summer**	**−0.27**	**0.025**

Overall, there was no significant correlation between the annual burned area and PDSI variables (the annual, spring, summer, maximum, minimum, median, standard deviation, and difference between the spring and summer PDSIs) for O'Higgins, Metropolitana, and Valparaíso Regions. Also, there was no association between the difference of spring and summer PDSI and area burned in any of the regions.

Although forest fires are complex processes driven by several variables, for La Araucanía and Maule, we found significant relationships between the area burned and maximum and summer PDSIs according to the regression analysis. Thus, the maximum PDSI was significantly related with the area burned in La Araucanía for 50–100 ha fires ($r^2 = 0.41$; $p < 0.05$) whereas the summer PDSI was associated better with fires smaller than 50 ha (r^2;0.29; $p < 0.05$) and fires greater than 100 ha ($r^2 = 0.21$; $p < 0.05$). For the Maule Region, 18% (for fires greater than 100 ha) and 29% (for fires smaller than 50 ha) of the variability of the burned area could be explained by the summer PDSI (Figure 8). Regardless of the regression model (linear or non-linear), drought and wildfires are negatively related to a lower PDSI (more severe drought) and associated with a greater burned area (Figure 8). In addition to La Araucanía and Maule, similar patterns were observed for Biobío and Ñuble Regions, although they were non-significant.

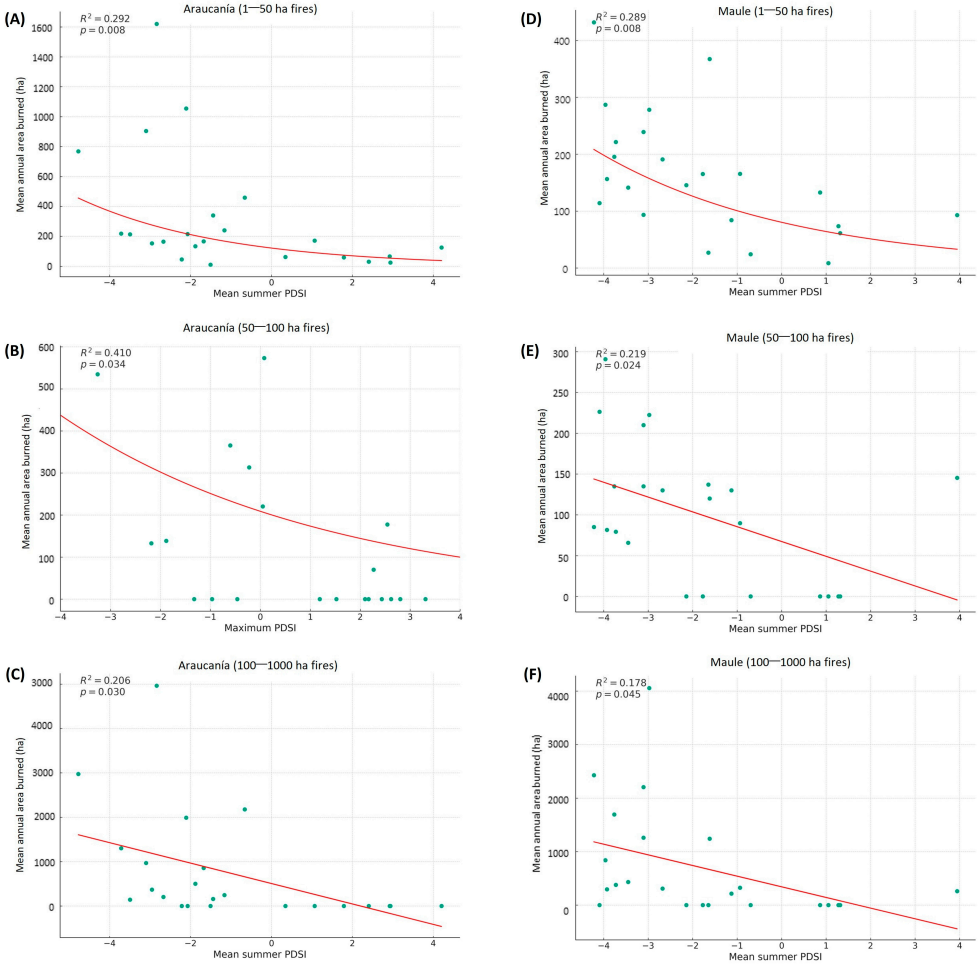

Figure 8. Regression analysis between annual mean burned area (ha) and maximum or summer Palmer Drought Severity Index (PDSI) for: (**A**) La Araucanía Region for 1−50 ha size fires, (**B**) La Araucanía Region for 50−100 ha size fires, (**C**) La Araucanía Region for 100−1000 ha size fires, (**D**) El Maule Region for 1−50 ha size fires, (**E**) El Maule Region for 50−1000 ha size fires, and (**F**) El Maule Region for 100−1000 ha size fires.

4. Discussion

The climate change predictions for central-southern Chile indicate that heat waves and droughts will be more frequent, intense, and of longer duration resulting in an increased risk of wildfires [52]. In this context, it is critical to understand and mitigate the effects of prolonged droughts [53]. This is particularly important considering the potential climate scenarios that may exacerbate such events and therefore, influence the wildfire dynamics in the forest ecosystems at a regional scale.

In this study, we showed a relationship between the long-term drought affecting the south-central region of Chile and the recurrence of native forest fires, which almost tripled the average annual area of native forest affected by fire before the drought period (2000–2006) and during the drought period (2007–2023). Understanding this relationship is critical for enhancing the wildfire prediction and management, prioritizing preventive measures, and allocating resources in vulnerable regions, thereby improving the resilience against climate-induced wildfire risks. This knowledge is essential for informing both local and global wildfire mitigation strategies.

4.1. Relationship between the PDSI and Forest Fire

Here, our hypothesis that the PDSI correlates with drought conditions and wildfire events across diverse ecosystems was successfully evaluated; a significant increase in fire

frequency and burned area with more severe drought was observed in Maule, Ñuble, Biobío, and La Araucanía. An increase in the burned area with increased drought had been previously reported for the Maule Region, while for La Araucanía, Ñuble, and Biobío, these increases had been non-significant until the year 2015 [1]. This is in line with our results, where a significant increase in the burned area in La Araucanía, Ñuble, and Biobío (Mediterranean climate with wet winters and dry summers) were exhibited only in the last period of severe drought (2019–2023).

In the regions more northern than Maule, the increase in drought severity did not increase the fire frequency and area burned according to the LSD test. Although a Mediterranean climate is found from Valparaíso to La Araucanía, this varies from semi-arid conditions in the north to more mesic and humid conditions in the south. Thus, the annual accumulated precipitation ranges from 150 to 200 mm in Valparaíso to 1000–2500 mm in La Araucanía [1,54].

The precipitation during the preceding one to two growing seasons influences the biomass production and fire activity [27]. Furthermore, the growing season precipitation has been identified as one of the most important predictors of fire likelihood in Chile [7], explaining why the long-term drought increased the fire frequency and area burned only in regions with mesic and humid conditions where precipitation seasonality promoted the growth of shrubs and grasses during the winter and spring that dried up during the summer (summer–dry climate) [14,15].

For a more arid Mediterranean climate (Valparaíso, Metropolitana, and O'Higgins Regions), a multi-year drought with a precipitation deficit of up to 50% since 2007 (16 consecutive years) limited rapidly growing fuel (grasses, herbs, and fast-growing shrubs) and reduced the risk of wildfires [55,56], presenting fewer fires and area burned, thus being less responsive to drought. Furthermore, the O'Higgins and Metropolitana Regions showed a weak, non-significant positive association between the PDSI and forest fire, suggesting that drought might even reduce the fire risk [55].

Conversely, the Los Ríos Region is characterized by a predominant marine west-coast climate with an annual precipitation exceeding 2000 mm [54]. In this region, there was no significant increase in burned area or fire frequency associated with the drought severity but there was a significant positive association between the maximum PDSI and area burned, similarly to the more arid Mediterranean climate regions. The maximum PDSI (less severe drought) does not reflect the conditions during the summer when most fires take place but might represent the pre-summer conditions (late winter and spring) that promote the growth of fine fuels and thus increase the wildfire risk in this region. Although the native forest affected by fires in the Los Ríos Region is less than 2% of the area affected in the mesic Mediterranean climate regions [13], it is essential to further study the association between drought and forest fire in this type of climate.

The summer and maximum PDSIs explain between 18 to 41% or the variability in the burned area in La Araucanía and Maule with no significant relationship for the other regions. These results suggest that while there is a positive association between drought and burned area (a greater drought is associated with a greater burned area) in the four regions, drought alone does not strongly predict the burned area in forest ecosystems of mesic Mediterranean climate regions. This highlights the differences within Mediterranean climate regions, suggesting that only regions with more mesic conditions might be vulnerable to higher fire risk under drought conditions.

Although drought is a contributing factor to fire frequency and burned area, drought acts in conjunction with a complex set of other variables including climatic, land cover, topographic, and human factors [3,7] that are specific to each site. Thus, other factors also influencing the burned area and fire frequency should be considered.

4.2. Native Forest Degradation

Forest degradation is the loss of biological or economic productivity or of a desired level of maintenance over time of floristic diversity, biotic integrity, and ecological pro-

cesses [57]. In Chile, 46,200 ha year^{-1} of degraded native forest during the period 2001–2010, including 8590 ha year^{-1} due to forest fires, have been reported [57].

It is estimated that CO_{2eq} emissions from the degradation of native forests represent 2.6 times more than the emissions caused by deforestation (loss of native forests to grasslands, shrublands, urban areas, and other uses [57]. In our study, we found that before the drought (2000–2006), an average of 8775 ha year^{-1} of native forest was degraded by fires, and during the drought (2007–2023), there was an average of 21,634 ha year^{-1}; the early successional forest was the most affected by fires in recent years with 334,410 ha equivalent to 82% of the total native forest affected by forest fires (2000–2023); these findings confirm that forest degradation is the largest cause of CO_2 emissions compared to emissions caused by deforestation or forest replacement [58–60].

The methodology applied in this study integrates satellite imagery with ground data, enhancing the precision in identifying areas of forests degraded by wildfires. Other models use satellite images (e.g., MODIS) and apply indirect estimates of forest degradation through time series using various vegetation indices, such as Near Infrared Reflectance of Vegetation (NIRv) [61], the Normalized Difference Vegetation Index (NDVI) [62], Enhanced Vegetation Index (EVI) [63], and Normalized Difference Fraction Index (NDFI) [64]). Due to their spatial and temporal resolution, Sentinel-2 images are increasingly used to monitor wildfires and forest degradation. Indices such as the differenced Normalized Burn Ratio (dNBR) have become standard tools for assessing the burn or fire severity across larger areas [65,66]. Additionally, to monitor the long-term vegetation dynamics, images from the Landsat satellite program are utilized [67]. For example, in the south-central region of Chile, Miranda et al. (2020) conducted a mapping of 8153 fire scars for the period 1985–2018 [68].

Although this study primarily focuses on the central-south macrozone of Chile, the findings have broader implications for similar bioclimatic regions worldwide (e.g., Mediterranean climate zones), where the increasing drought severity and wildfire frequency pose significant threats to forest ecosystems. Future research could extend this study by exploring the applicability of these methods in different climatic and ecological contexts, examining the long-term impacts of forest degradation and CO_2 emissions caused by wildfires.

5. Conclusions

(i) The frequency of fires and the extent of area burned within native forests have escalated with the intensification of drought conditions throughout the beginning of the 21st century. However, the response to drought appears to be modulated by the dominant macroclimatic conditions. For example, the relationship between drought intensity and wildfire incidence was observed in the mesic to humid Mediterranean climatic regions of Maule, Biobío, Ñuble, and La Araucanía, where seasonal precipitation patterns, particularly during the winter and spring, foster the proliferation of shrubs and grasses, and these fine fuels substantially elevate the risk of fire ignition and propagation. **(ii)** Integrating satellite-derived datasets, particularly from the MODIS instrument, significantly enhances wildfire research by providing scalable observations of fire events and post-burn vegetation recovery. This approach facilitates an understanding of the spatial and temporal dynamics of wildfires. **(iii)** The advanced information technologies applied in this study have yielded high precision in correlating in situ data with satellite-based wildfire observations, underscoring the reliability of remote sensing as a tool for ecological monitoring and assessment. **(iv)** This study introduces a novel approach by combining long-term drought indices with satellite imagery to assess the impact of climate variability on the wildfire dynamics in native forests. The integration of remote sensing data with ground-based observations provides a robust framework for monitoring and understanding the wildfire behavior in response to the changing climatic conditions. **(v)** Further research should explore the application of these methods in different climatic and ecological contexts to further validate their efficacy. Additionally, examining the long-term impacts of forest degradation and carbon emissions due to wildfires will provide deeper insights into the ecological consequences of climate change. **(vi)** The findings of this study have significant implications

for the policy formulation aimed at mitigating the risks of forest fires, drought, and land degradation. It is essential to develop and implement comprehensive land management strategies that integrate advanced remote sensing technologies. These technologies can be used to design effective prevention strategies at various territorial scales, enhancing the ability to anticipate and respond to environmental challenges.

Author Contributions: Conceptualization, E.D.; methodology, E.D. and C.G.-R.; validation, E.D. and C.G.-R.; formal analysis, E.D. and C.G.-R.; investigation, E.D., R.R. and C.G.-R.; data curation, E.D.; writing—original draft preparation, E.D. and C.G.-R.; writing—review and editing, E.D., C.G.-R., R.R., F.M., C.M., C.S.-R., F.A., C.R., A.S., J.D., F.N., G.B. and I.J. All authors have read and agreed to the published version of the manuscript.

Funding: This research was funded by ANID-Chile, project ANID-ANILLO ACT210060: FiRING: Multiscale effects of extreme wildfires on soil, water, biogeochemical cycling, and erosion in natural and managed forests.

Institutional Review Board Statement: Not applicable.

Informed Consent Statement: Not applicable.

Data Availability Statement: The data that support the findings of this study are available from the corresponding author, [E.D.], upon reasonable request.

Acknowledgments: The authors acknowledge that the Associative Research Program from ANID-Chile is financing the project titled "FiRING: Multiscale effects of extreme wildfires on soil, water, biogeochemical cycling and erosion in natural and managed forests", Project ANID—ANILLO ACT210060, the ANID Basal Project FB210015—Centro Nacional de Excelencia para la Industria de la Madera (CENAMAD), and the ANID FB210006 project.

Conflicts of Interest: The authors declare no conflicts of interest.

Appendix A

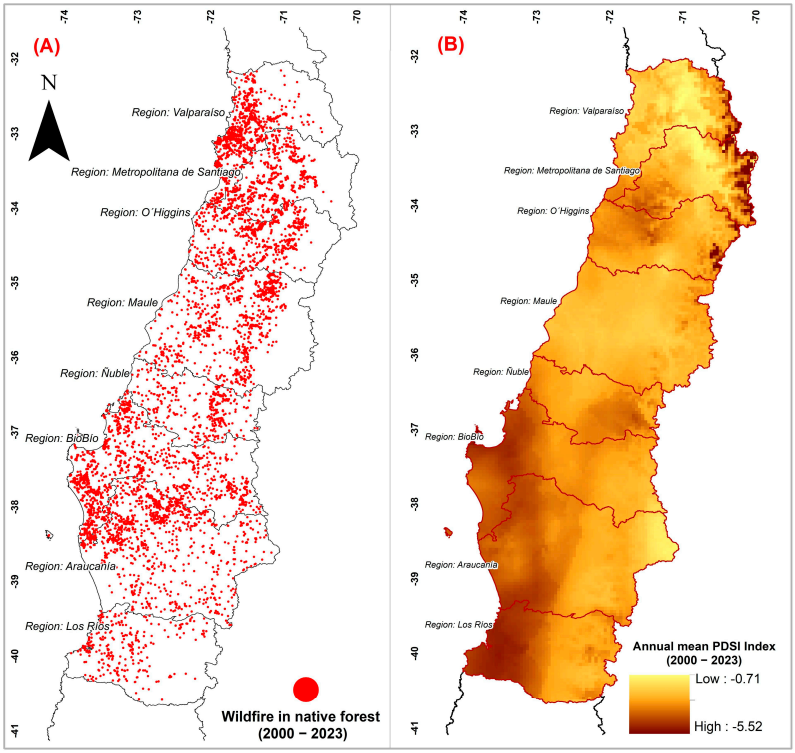

Figure A1. (**A**) National wildfire database (2000−2023) and (**B**) Annual mean PDSI Index 2000−2023.

Appendix B

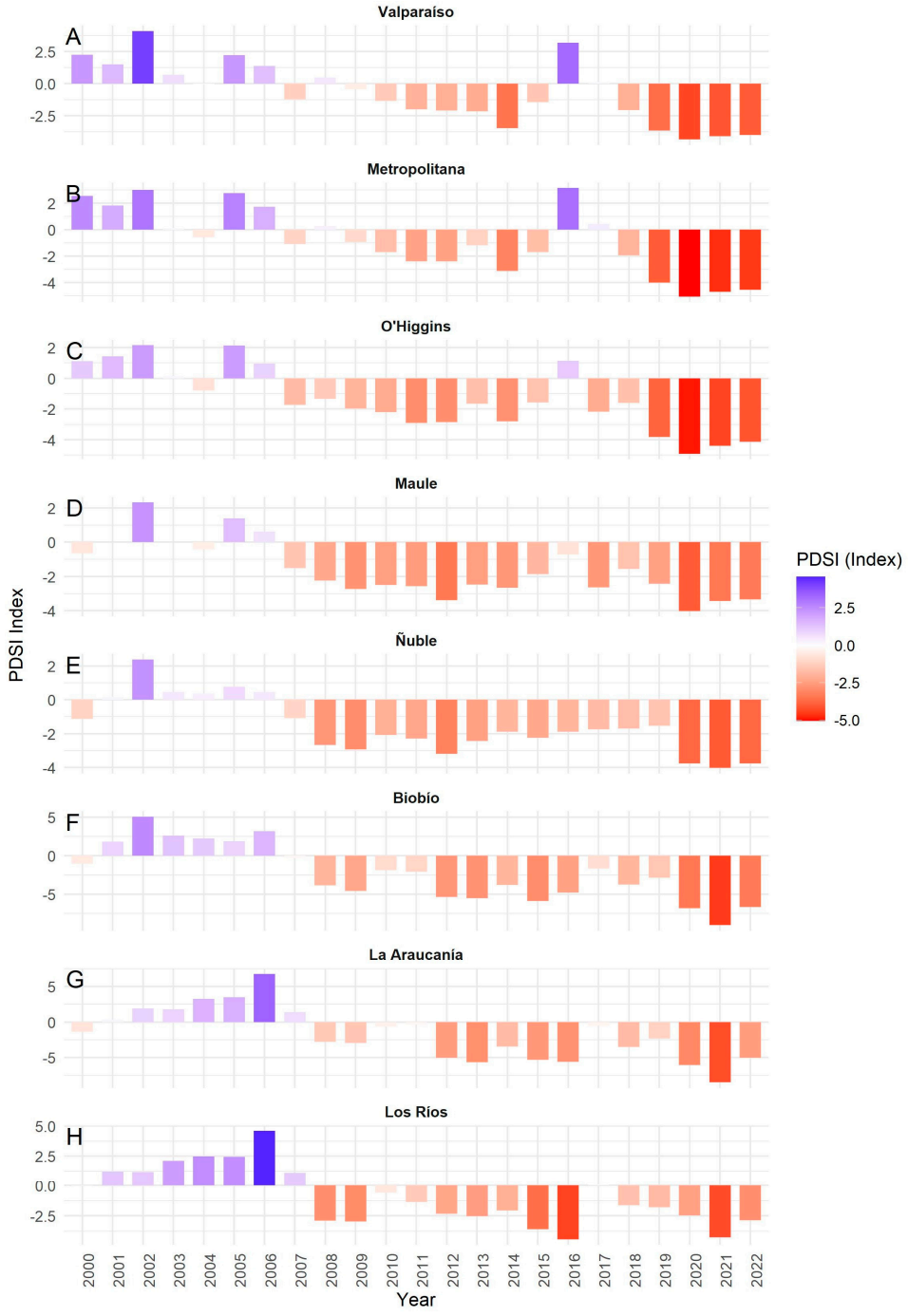

Figure A2. PDSI values for each region for the years 2000 to 2023. (**A**) = Valparaíso: Alternating between wet and dry; persistent drought since 2010. (**B**) Metropolitana: Predominantly dry since 2007, severe since 2014. (**C**) O'Higgins: Drought since 2007, intense since 2013. (**D**) Maule: Persistent drought since 2007, severe since 2010. (**E**) Ñuble: Continuous drought since 2007, more severe since 2010. (**F**) Biobío: Dry since mid-2000s, severe since 2012. (**G**) La Araucanía: Wet until 2006, severe drought since 2014. (**H**) Los Ríos: Wet until 2006, intense drought since 2013.

References

1. González, M.E.; Gómez-González, S.; Lara, A.; Garreaud, R.; Díaz-Hormazábal, I. The 2010–2015 Megadrought and its influence on the fire regime in central and south-central Chile. *Ecosphere* **2018**, *9*, e02300. [CrossRef]
2. Halofsky, J.E.; Peterson, D.L.; Harvey, B.J. Changing wildfire, changing forests: The effects of climate change on fire regimes and vegetation in the Pacific Northwest, USA. *Fire Ecol.* **2020**, *16*, 4. [CrossRef]
3. Littell, J.S.; Peterson, D.L.; Riley, K.L.; Liu, Y.; Luce, C.H. A review of the relationships between drought and forest fire in the United States. *Glob. Change Biol.* **2016**, *22*, 2353–2369. [CrossRef] [PubMed]
4. Wasserman, T.N.; Mueller, S.E. Climate influences on future fire severity: A synthesis of climate-fire interactions and impacts on fire regimes, high-severity fire, and forests in the western United States. *Fire Ecol.* **2023**, *19*, 43. [CrossRef]
5. Tyukavina, A.; Potapov, P.; Hansen, M.C.; Pickens, A.H.; Stehman, S.V.; Turubanova, S.; Parker, D.; Zalles, V.; Lima, A.; Kommareddy, I.; et al. Global Trends of Forest Loss Due to Fire From 2001 to 2019. *Front. Remote Sens.* **2022**, *3*, 825190. [CrossRef]
6. Boer, M.M.; Resco de Dios, V.; Bradstock, R.A. Unprecedented burn area of Australian mega forest fires. *Nat. Clim. Change* **2020**, *10*, 171–172. [CrossRef]
7. McWethy, D.B.; Pauchard, A.; García, R.A.; Holz, A.; González, M.E.; Veblen, T.T.; Stahl, J.; Currey, B. Landscape drivers of recent fire activity (2001–2017) in south-central Chile. *PLoS ONE* **2018**, *13*, e0201195. [CrossRef]
8. Heilmayr, R.; Echeverría, C.; Fuentes, R.; Lambin, E.F. A plantation-dominated forest transition in Chile. *Appl. Geogr.* **2016**, *75*, 71–82. [CrossRef]
9. Garrido-Ruiz, C.; Sandoval, M.; Stolpe, N.; Sanchez-Hernandez, J.C. Fire impacts on soil and post fire emergency stabilization treatments in Mediterranean-climate regions. *Chil. J. Agric. Res.* **2022**, *82*, 335–347. [CrossRef]
10. Garreaud, R.D.; Boisier, J.P.; Rondanelli, R.; Montecinos, A.; Sepúlveda, H.H.; Veloso-Aguila, D. The Central Chile Mega Drought (2010–2018): A climate dynamics perspective. *Int. J. Climatol.* **2020**, *40*, 421–439. [CrossRef]
11. Alvarez-Garreton, C.; Boisier, J.P.; Garreaud, R.; Seibert, J.; Vis, M. Progressive water deficits during multiyear droughts in basins with long hydrological memory in Chile. *Hydrol. Earth Syst. Sci.* **2021**, *25*, 429–446. [CrossRef]
12. Barrientos, G.; Rubilar, R.; Duarte, E.; Paredes, A. Runoff variation and progressive aridity during drought in catchments in southern-central Chile. *Hydrol. Res.* **2023**, *54*, 1590–1605. [CrossRef]
13. CONAF. Estadísticas Históricas: Incendios Forestales. Estadísticas Históricas de Incendios Forestales en Chile. 2023. Available online: http://www.conaf.cl/incendios-forestales/incendios-forestales-en-chile/estadisticas-historicas/ (accessed on 17 December 2021).
14. Bowman, D.M.J.S.; Moreira-Muñoz, A.; Kolden, C.A.; Chávez, R.O.; Muñoz, A.A.; Salinas, F.; González-Reyes, Á.; Rocco, R.; de la Barrera, F.; Williamson, G.J.; et al. Human–environmental drivers and impacts of the globally extreme 2017 Chilean fires. *Ambio* **2019**, *48*, 350–362. [CrossRef] [PubMed]
15. Urrutia-Jalabert, R.; González, M.E.; González-Reyes, Á.; Lara, A.; Garreaud, R. Climate variability and forest fires in central and south-central Chile. *Ecosphere* **2018**, *9*, e02171. [CrossRef]
16. Piao, Y.; Lee, D.; Park, S.; Kim, H.G.; Jin, Y. Multi-hazard mapping of droughts and forest fires using a multi-layer hazards approach with machine learning algorithms. *Geomat. Nat. Hazards Risk* **2022**, *13*, 2649–2673. [CrossRef]
17. Scasta, J.D.; Weir, J.R.; Stambaugh, M.C. Droughts and Wildfires in Western U.S. Rangelands. *Rangelands* **2016**, *38*, 197–203. [CrossRef]
18. Torres, P.; Rodes-Blanco, M.; Viana-Soto, A.; Nieto, H.; García, M. The Role of Remote Sensing for the Assessment and Monitoring of Forest Health: A Systematic Evidence Synthesis. *Forests* **2021**, *12*, 1134. [CrossRef]
19. Payra, S.; Sharma, A.; Verma, S. Chapter 14—Application of remote sensing to study forest fires. In *Atmospheric Remote Sensing*; Kumar Singh, A., Tiwari, S., Eds.; Elsevier: Amsterdam, The Netherlands, 2023; pp. 239–260.
20. Vo, V.D.; Kinoshita, A.M. Remote sensing of vegetation conditions after post-fire mulch treatments. *J. Environ. Manag.* **2020**, *260*, 109993. [CrossRef] [PubMed]
21. Pérez-Cabello, F.; Montorio, R.; Alves, D.B. Remote sensing techniques to assess post-fire vegetation recovery. *Curr. Opin. Environ. Sci. Health* **2021**, *21*, 100251. [CrossRef]
22. Bar, S.; Parida, B.R.; Pandey, A.C. Landsat-8 and Sentinel-2 based Forest fire burn area mapping using machine learning algorithms on GEE cloud platform over Uttarakhand, Western Himalaya. *Remote Sens. Appl. Soc. Environ.* **2020**, *18*, 100324. [CrossRef]
23. Saleh, A.; Zulkifley, M.A.; Harun, H.H.; Gaudreault, F.; Davison, I.; Spraggon, M. Forest fire surveillance systems: A review of deep learning methods. *Heliyon* **2024**, *10*, e23127. [CrossRef] [PubMed]
24. Palmer, W.C. *Meteorological Drought*; U.S. Department of Commerce, Weather Bureau: Silver Spring, MD, USA, 1965.
25. Zhao, F.; Liu, Y. Important meteorological predictors for long-range wildfires in China. *For. Ecol. Manag.* **2021**, *499*, 119638. [CrossRef]
26. Donovan, V.M.; Wonkka, C.L.; Wedin, D.A.; Twidwell, D. Land-Use Type as a Driver of Large Wildfire Occurrence in the U.S. Great Plains. *Remote Sens.* **2020**, *12*, 1869. [CrossRef]
27. Yang, S.; Zeng, A.; Tigabu, M.; Wang, G.; Zhang, Z.; Zhu, H.; Guo, F. Investigating Drought Events and Their Consequences in Wildfires: An Application in China. *Fire* **2023**, *6*, 223. [CrossRef]
28. Peel, M.C.; Finlayson, B.L.; McMahon, T.A. Updated world map of the Köppen-Geiger climate classification. *Hydrol. Earth Syst. Sci.* **2007**, *11*, 1633–1644. [CrossRef]

29. CONAF. Cifras Oficiales y Actualizadas Provenientes del Catastro de los Recursos Vegetacionales y Uso de la Tierra. 2023. Available online: https://www.conaf.cl/nuestros-bosques/bosques-en-chile/catastro-vegetacional/ (accessed on 1 February 2024).
30. Donoso, P.; Promis, A. Forestry in Native Forests. Advances in research in Chile, Argentina and New Zeland. In *Las Especies Arbóreas de Los Bosques Templados de Chile Y Argentina*; Marisa Cuneo Ediciones: Valdivia, Chile, 2013.
31. Holz, A.; Haberle, S.; Veblen, T.T.; de Pol-Holz, R.; Southon, J. Fire history in western Patagonia from paired tree-ring fire-scar and charcoal records. *Clim. Past* **2012**, *8*, 451–466. [CrossRef]
32. Veblen, T.T.; Donoso, C.; Kitzberger, T.; Rebertus, A. Ecology of Southern Chilean and Argentinean Nothofagus Forest. In *Ecology and Biogeography of Nothofagus Forest*; Yale University Press: London, UK, 1996.
33. Gonzáles, M.; Cortés, M.; Izquierdo, F.; Gallo, L.; Echeverría, C.; Bekessy, C. Araucaria araucana. In *Las Especies Arbóreas de Los Bosques Templados de Chile Y Argentina, Autoecología*; Biblioteca Digital Instituto Forestal: Concepción, Chile, 2013; pp. 36–53.
34. Gorelick, N.; Hancher, M.; Dixon, M.; Ilyushchenko, S.; Thau, D.; Moore, R. Google Earth Engine: Planetary-scale geospatial analysis for everyone. *Remote Sens. Environ.* **2017**, *202*, 18–27. [CrossRef]
35. Giglio, L.; Justice, C.; Boschetti, L.; Roy, D. *MODIS/Terra + Aqua Burned Area Monthly L3 Global 500m SIN Grid V061 [Data Set]*; USGS: Reston, VA, USA, 2021. [CrossRef]
36. Liu, Y.; Zhu, Y.; Ren, L.; Singh, V.P.; Yang, X.; Yuan, F. A multiscalar Palmer drought severity index. *Geophys. Res. Lett.* **2017**, *44*, 6850–6858. [CrossRef]
37. Abatzoglou, J.T.; Dobrowski, S.Z.; Parks, S.A.; Hegewisch, K.C. TerraClimate, a high-resolution global dataset of monthly climate and climatic water balance from 1958–2015. *Sci. Data* **2018**, *5*, 170191. [CrossRef]
38. Rhee, J.; Carbone, G.J. A Comparison of Weekly Monitoring Methods of the Palmer Drought Index. *J. Clim.* **2007**, *20*, 6033–6044. [CrossRef]
39. Dai, A. (Ed.); NCAR. The Climate Data Guide: Palmer Drought Severity Index (PDSI). 2024. Available online: https://climatedataguide.ucar.edu/climate-data/palmer-drought-severity-index-pdsi (accessed on 1 February 2024).
40. NOAA; CPC. Weekly Palmer Drought and Crop Moisture Data Products Explanation. 2024. Available online: https://www.cpc.ncep.noaa.gov/products/analysis_monitoring/cdus/palmer_drought/wpdanote.shtml (accessed on 1 February 2024).
41. Dai, A. Characteristics and trends in various forms of the Palmer Drought Severity Index during 1900–2008. *J. Geophys. Res. Atmos.* **2011**, *116*. [CrossRef]
42. Szép, I.J.; Mika, J.; Dunkel, Z. Palmer drought severity index as soil moisture indicator: Physical interpretation, statistical behaviour and relation to global climate. *Phys. Chem. Earth Parts A/B/C* **2005**, *30*, 231–243. [CrossRef]
43. Nkemdirim, L.C. PALMER DROUGHT INDEX. In *Encyclopedia of Atmospheric Sciences*; Holton, J.R., Ed.; Academic Press: Oxford, UK, 2003; pp. 1685–1691.
44. Wells, N.; Goddard, S.; Hayes, M.J. A Self-Calibrating Palmer Drought Severity Index. *J. Clim.* **2004**, *17*, 2335–2351. [CrossRef]
45. Wang-Erlandsson, L.; Bastiaanssen, W.G.M.; Gao, H.; Jägermeyr, J.; Senay, G.B.; van Dijk, A.I.J.M.; Guerschman, J.P.; Keys, P.W.; Gordon, L.J.; Savenije, H.H.G. Global root zone storage capacity from satellite-based evaporation. *Hydrol. Earth Syst. Sci.* **2016**, *20*, 1459–1481. [CrossRef]
46. Liu, C.; Yang, C.; Yang, Q.; Wang, J. Spatiotemporal drought analysis by the standardized precipitation index (SPI) and standardized precipitation evapotranspiration index (SPEI) in Sichuan Province, China. *Sci. Rep.* **2021**, *11*, 1280. [CrossRef]
47. Beguería, S.; Vicente—Serrano, S.M.; Reig, F.; Latorre, B. Standardized precipitation evapotranspiration index (SPEI) revisited: Parameter fitting, evapotranspiration models, tools, datasets and drought monitoring. *Int. J. Climatol.* **2014**, *34*, 3001–3023. [CrossRef]
48. Rayne, S.; Forest, K. Evidence for increasingly variable palmer drought severity index in the United States since 1895. *Sci. Total Environ.* **2016**, *544*, 792–796. [CrossRef]
49. CONAF. Catastro de los Recursos Vegetacionales Nativos de Chile al año 2020. 2021; Volume 76. Available online: https://sit.conaf.cl/varios/Catastros_Recursos_Vegetacionales_Nativos_de_Chile_Nov2021.pdf (accessed on 1 February 2024).
50. Tedim, F.; Leone, V.; Amraoui, M.; Bouillon, C.; Coughlan, M.R.; Delogu, G.M.; Fernandes, P.M.; Ferreira, C.; McCaffrey, S.; McGee, T.K. Defining extreme wildfire events: Difficulties, challenges, and impacts. *Fire* **2018**, *1*, 9. [CrossRef]
51. Nolan, R.H.; Boer, M.M.; Collins, L.; Resco de Dios, V.; Clarke, H.; Jenkins, M.; Kenny, B.; Bradstock, R.A. Causes and consequences of eastern Australia's 2019-20 season of mega-fires. *Glob. Change Biol.* **2020**, *26*, 1039–1041. [CrossRef] [PubMed]
52. Pica-Téllez, A.; Garreaud, R.; Meza, F.; Bustos, S.; Falvey, M.; Ibarra, M.; Duarte, K.; Ormazábal, R.; Dittborn, R.; Silva, I. *Informe Proyecto ARClim: Atlas de Riesgos Climáticos Para Chile*; Centro de Ciencia del Clima y la Resiliencia, Centro de Cambio Global UC and Meteodata for the Ministerio del Medio Ambiente via La Deutsche Gesellschaft für Internationale Zusammenarbeit (GIZ): Santiago, Chile, 2020.
53. Garreaud, R.D.; Alvarez-Garreton, C.; Barichivich, J.; Boisier, J.P.; Christie, D.; Galleguillos, M.; LeQuesne, C.; McPhee, J.; Zambrano-Bigiarini, M. The 2010–2015 megadrought in central Chile: Impacts on regional hydroclimate and vegetation. *Hydrol. Earth Syst. Sci.* **2017**, *21*, 6307–6327. [CrossRef]
54. Araya-Osses, D.; Casanueva, A.; Román-Figueroa, C.; Uribe, J.M.; Paneque, M. Climate change projections of temperature and precipitation in Chile based on statistical downscaling. *Clim. Dyn.* **2020**, *54*, 4309–4330. [CrossRef]
55. Davis, A.; MacAfee, S.; Restaino, C.; Ormerod, K.J. Drought and Fire in Nevada: Is Fire Risk Higher during Drought? 2022. Available online: https://extension.unr.edu/publication.aspx?PubID=4950 (accessed on 19 October 2023).

56. Villaroel, C.; Gutierrez, R.; Aravena, C.; Gotelli, C.; Vásquez, R.; Vilches, C. *Reporte Anual de la Evolución del Chile en Chile 2022*; Meteorological Directorate of Chile: Santiago, Chile, 2023; p. 52.
57. CONAF. Estrategia Nacional de Cambio Climático y Recursos Vegetacionales ENCCRV. 2016. Available online: https://www.conaf.cl/cms/editorweb/ENCCRV/ENCCRV-3a_Edicion-17mayo2017.pdf (accessed on 1 February 2024).
58. Qin, Y.; Xiao, X.; Wigneron, J.-P.; Ciais, P.; Brandt, M.; Fan, L.; Li, X.; Crowell, S.; Wu, X.; Doughty, R.; et al. Carbon loss from forest degradation exceeds that from deforestation in the Brazilian Amazon. *Nat. Clim. Change* **2021**, *11*, 442–448. [CrossRef]
59. Duarte, E.; Barrera, J.A.; Dube, F.; Casco, F.; Hernández, A.J.; Zagal, E. Monitoring Approach for Tropical Coniferous Forest Degradation Using Remote Sensing and Field Data. *Remote Sens.* **2020**, *12*, 2531. [CrossRef]
60. Pearson, T.R.H.; Brown, S.; Murray, L.; Sidman, G. Greenhouse gas emissions from tropical forest degradation: An underestimated source. *Carbon Balance Manag.* **2017**, *12*, 3. [CrossRef] [PubMed]
61. Badgley, G.; Field, C.B.; Berry, J.A. Canopy near-infrared reflectance and terrestrial photosynthesis. *Sci. Adv.* **2017**, *3*, e1602244. [CrossRef] [PubMed]
62. Sobrino, J.A.; Raissouni, N. Toward remote sensing methods for land cover dynamic monitoring: Application to Morocco. *Int. J. Remote Sens.* **2000**, *21*, 353–366. [CrossRef]
63. Huete, A.R.; Liu, H.Q.; Batchily, K.; van Leeuwen, W. A comparison of vegetation indices over a global set of TM images for EOS-MODIS. *Remote Sens. Environ.* **1997**, *59*, 440–451. [CrossRef]
64. Souza, C.M.; Roberts, D.A.; Cochrane, M.A. Combining spectral and spatial information to map canopy damage from selective logging and forest fires. *Remote Sens. Environ.* **2005**, *98*, 329–343. [CrossRef]
65. Viedma, O.; Chico, F.; Fernández, J.J.; Madrigal, C.; Safford, H.D.; Moreno, J.M. Disentangling the role of prefire vegetation vs. burning conditions on fire severity in a large forest fire in SE Spain. *Remote Sens. Environ.* **2020**, *247*, 111891. [CrossRef]
66. Fassnacht, F.E.; Schmidt-Riese, E.; Kattenborn, T.; Hernández, J. Explaining Sentinel 2-based dNBR and RdNBR variability with reference data from the bird's eye (UAS) perspective. *Int. J. Appl. Earth Obs. Geoinf.* **2021**, *95*, 102262. [CrossRef]
67. Wulder, M.A.; Loveland, T.R.; Roy, D.P.; Crawford, C.J.; Masek, J.G.; Woodcock, C.E.; Allen, R.G.; Anderson, M.C.; Belward, A.S.; Cohen, W.B.; et al. Current status of Landsat program, science, and applications. *Remote Sens. Environ.* **2019**, *225*, 127–147. [CrossRef]
68. Miranda, A.; Mentler, R.; Moletto-Lobos, Í.; Alfaro, G.; Aliaga, L.; Balbontín, D.; Barraza, M.; Baumbach, S.; Calderón, P.; Cárdenas, F.; et al. The Landscape Fire Scars Database: Mapping historical burned area and fire severity in Chile. *Earth Syst. Sci. Data* **2022**, *14*, 3599–3613. [CrossRef]